Received: 3 February 2020 | Accepted: 21 May 2020

DOI: 10.1002/jcp.29837

ORIGINAL RESEARCH ARTICLE

Journal of Cellular Physiology WILEY

Prognostic model and nomogram construction based on autophagy signatures in lower grade glioma

Chunhui Wang[1] | Jiting Qiu[2] | Sarah Chen[3] | Ying Li[4] | Hongkang Hu[1] | Yu Cai[2] | Lijun Hou[1]

[1]Department of Neurosurgery, Changzheng Hospital, Second Military Medical University, Shanghai, China

[2]Department of Neurosurgery, Ruijin Hospital North, Shanghai Jiaotong University School of Medicine, Shanghai, China

[3]University of North Carolina at Chapel Hill School of Medicine, Chapel Hill, North Carolina

[4]Department of Pathology, Changzheng Hospital, Second Military Medical University, Shanghai, China

Correspondence
Lijun Hou, Department of Neurosurgery, Changzheng Hospital, Second Military Medical University, 200003 Shanghai, China.
Email: lijunhou@smmu.edu.cn

Abstract

The median survival time of lower grade glioma (LGG) tumors spans a wide range of 2–10 years and is highly dependent on the molecular characteristics and tumor location. Currently, there is no prognostic predictor for these tumors based on autophagy-related (ATG) genes. A prognostic risk score model based on the most significant seven ATG genes was established for LGG. These seven genes, including GRID2, FOXO1, MYC, PTK6, IKBKE, BIRC5, and TP73, have been screened as potentially therapeutic targets. The Kaplan–Meier survival curve analyses validated that patients with high or low risk scores had significantly different overall survival. Following the multivariate Cox regression and area under the ROC curve (AUC) analysis, a final prognostic model based on age, World Health Organization grade, 1p19q-codeletion status, and ATG risk score was performed as an independent prognostic indicator (training set: $p = 4.09E{-}05$, AUC = 0.901; validation set-1: $p = .00069$, AUC = 0.808; validation set-2: $p = .0376$, AUC = 0.830). Subsequently, a prognostic nomogram was constructed for individualized survival prediction. The calibration plots showed excellent predict efficiency between probability and actual overall survival. In this study, we provided several potential biomarkers for further developing potentially therapeutic targets of LGG. We also established a prognostic model and nomogram to improve the clinical glioma management and assist individualized survival prediction.

KEYWORDS

autophagy signature, autophagy-related gene, lower grade glioma, nomogram, prognostic model

1 | INTRODUCTION

Lower grade glioma (LGG) is categorized as diffuse and anaplastic gliomas (including World Health Organization [WHO] Grades II and III, astrocytoma and oligodendroglioma; Furnari et al., 2007). Despite aggressive therapeutic strategies, such as neurosurgical resection, radiotherapy, and chemotherapy, patients with LGG have a median survival time of 2–10 years depending on the age of the patient, the

Abbreviations: ATG, autophagy-related; AUC, area under the ROC curve; CGGA, Chinese Glioma Genome Atlas; DE-ATGs, differentially expressed ATG genes; FDR, false discovery rate; GBM, glioblastoma multiforme; GO, Gene Ontology; GSEA, gene set enrichment analysis; GTEx, Genotype-Tissue Expression Database; HADb, Human Autophagy Database; KEGG, Kyoto Encyclopedia of Genes and Genomes; K-M, Kaplan–Meier; LASSO, the least absolute shrinkage and selection operator; LGG, lower grade glioma; OS, overall survival; ROC, receiver-operator characteristic curve; TCGA, The Cancer Genome Atlas.

Chunhui Wang and Jiting Qiu are co-first authors.

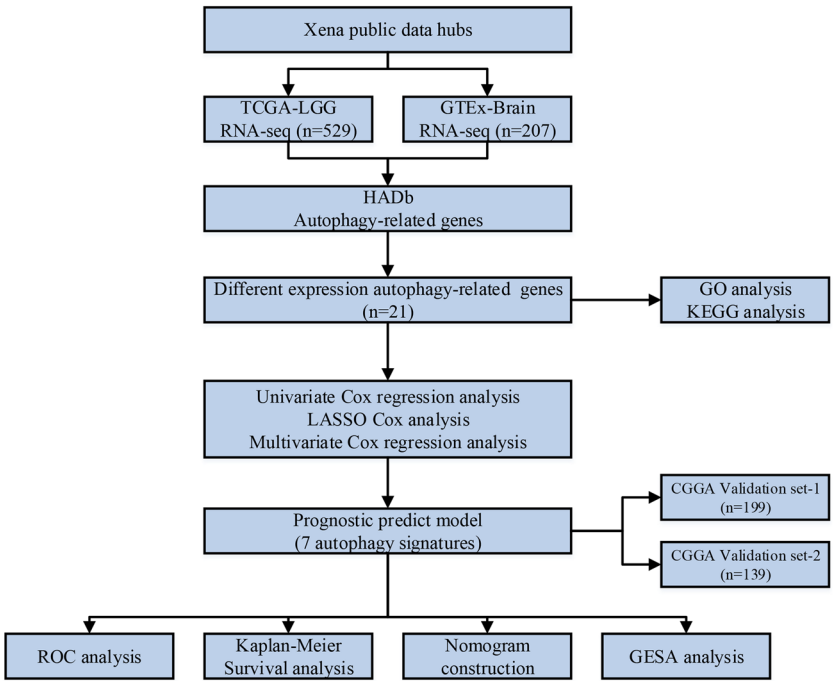

FIGURE 1 Flowchart for profiling the autophagy-related genes of LGG. Abbreviations: CGGA, Chinese Glioma Genome Atlas; CI, confidence interval; GESA, gene set enrichment analysis; GTEx, Genotype-Tissue Expression; HADb, Human Autophagy Database; ILASSO, least absolute shrinkage and selection operator; LGG, lower grade glioma; ROC, receiver operating characteristic; TCGA, The Cancer Genome Atlas

molecular features, and tumor location (Bauchet & Ostrom, 2019; Bready & Placantonakis, 2019).

Beyond mutant isocitrate dehydrogenase (IDH) and 1p/19q co-deletion, there is a lack of promising biomarkers and comprehensive models to predict clinical outcomes in patients with LGG (van den Bent, 2010). Recent studies have attempted to characterize the molecular basis for the histological and prognostic differences between LGG and glioblastoma multiforme (GBM; Rao, Santosh, & Somasundaram, 2010). However, with improvements in bioinformatics approaches, the use of novel biomarkers to precisely identify biologic classes of LGG become possible. Profiling studies have also led to the development of novel categorized methods based on the molecular profile identified by using various bioinformatic analysis (Petalidis et al., 2008).

Autophagy is the natural and regulated mechanism of the cell that removes unnecessary or dysfunctional cargo. The lysosomal degradation pathway mediated by autophagy-related (ATG) genes plays a fundamental role in cellular, tissue, and organismal homeostasis including removal of dangerous cargo, renovation during differentiation, and prevention of genomic damage in cancer (Levine & Kroemer, 2019). The theoretical supports of ATG genes in pathogenesis have been completed gradually in biological processes (Mizushima, 2018; Ulasov, Fares, Timashev, & Lesniak, 2019). To further elucidate potential progressive processes, screening novel biomarkers and constructing a prognostic model are essential.

To the best of our knowledge, there is no study to date that has constructed a prognostic model for LGG. We constructed an efficient, prognostically significant model composed of autophagy signatures, and a promising nomogram to assess patients' prognosis of LGG.

2 | METHODS

2.1 | Data retrieval and processing

The training set of LGG including RNA-sequencing data and corresponding clinical information was downloaded from The Cancer

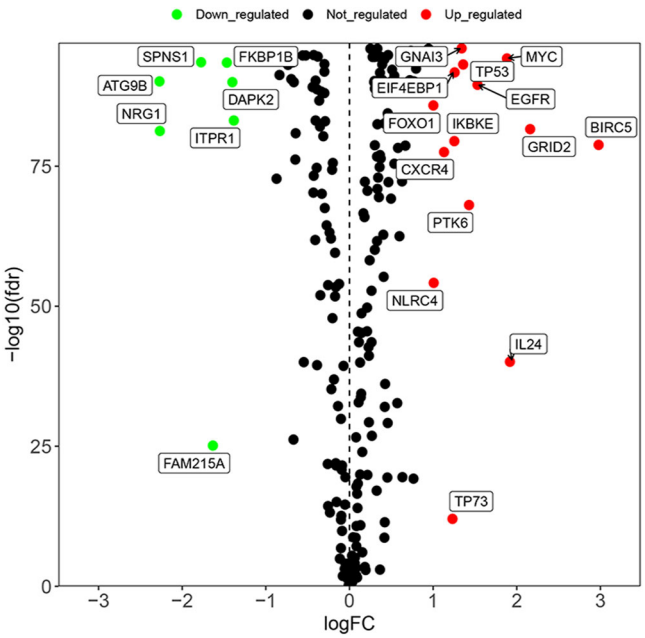

FIGURE 2 Volcano plot of differentially expressed ATG genes between the LGG samples from TCGA database and normal samples from GTEx database. ATG, autophagy-related; GTEx, Genotype-Tissue Expression Database; LGG, lower grade glioma; TCGA, The Cancer Genome Atlas

Genome Atlas (TCGA; https://tcga-data.nci.nih.gov/tcga/). Two validation sets of patients with LGG were downloaded from the Chinese Glioma Genome Atlas (CGGA; http://www.cgga.org.cn/). For differentially expressed analysis of ATG genes, the normal brain tissues were downloaded from the Genotype-Tissue Expression (GTEx) Database (https://www.gtexportal.org/). The expression levels of fragments per kilobase of exon model per million reads mapped (FPKM) data were log-transformed by log2 (FPKM + 1) for subsequent analysis. And the batch effects among different datasets were adjusted by the ComBat method with using R package "sva." The ATG genes of all tissue were obtained in the Human Autophagy Database (HADb; http://autophagy.lu/). Only cases with the primary tumor, postoperative overall survival (OS) of more than 30 days and with no adjuvant therapy preoperatively were included in our study. The schematic of the analysis flowchart is shown in Figure 1. All analyses were performed using R under version 3.5.1.

2.2 | Identification of differentially expressed ATG genes and enrichment analysis

The differentially expressed ATG genes (DE-ATGs) between the LGG and normal samples were identified by the Wilcox test. Adjusted *p* values (adj. *p*) were applied to correct the false-positive results by using the false discovery rate (FDR) method (Benjamini & Hochberg, 1995). Adj. $p < .05$ and $|\text{fold change (FC)}| > 1$ were considered the cutoff values for identifying DE-ATGs (Wang et al., 2019).

Here, we figure the volcano plot to show the DE-ATGs of TCGA. A total of 214 ATG genes, from HADb, provide a complete list of human genes and proteins in autophagy as described in the literature from PubMed and other public biological Databases (Moussay et al., 2011). The DE-ATGs that were considered significant for further analysis were then visualized by heat map analysis.

To better explore the biological mechanism associated with DE-ATGs, the functional annotation and pathway enrichment analyses of

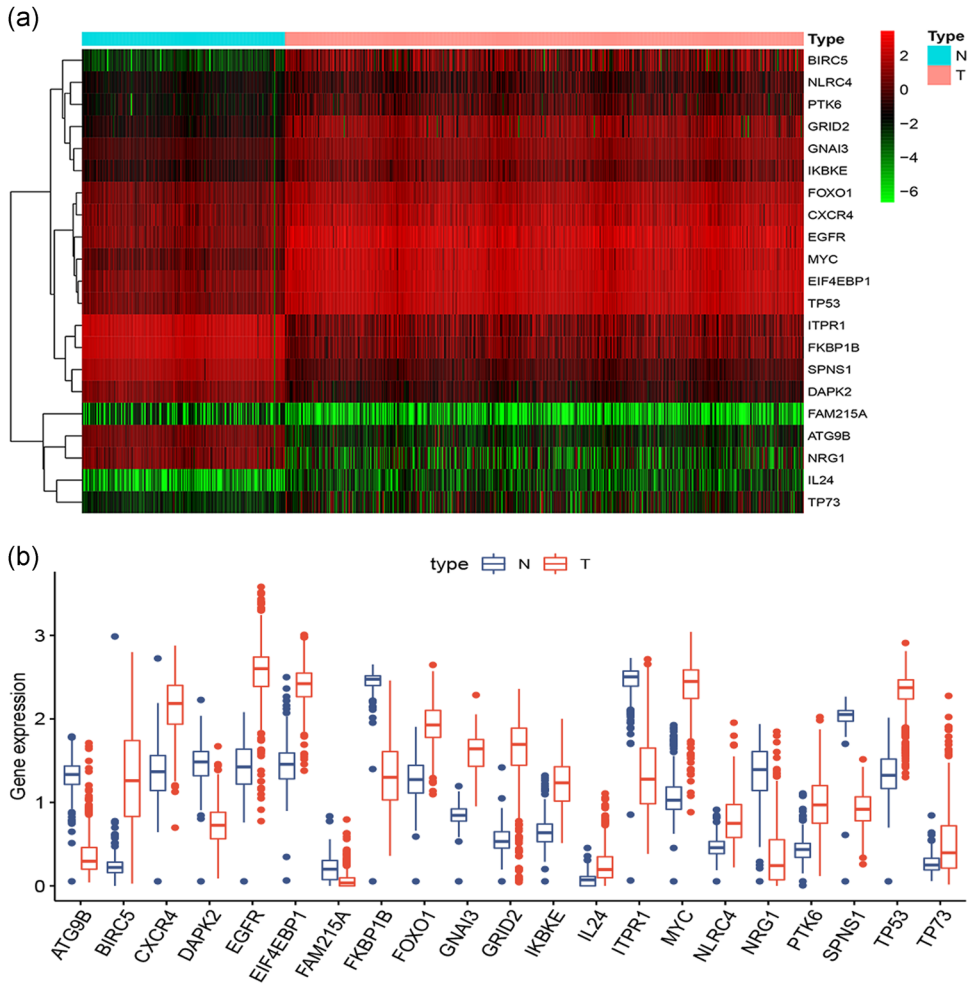

FIGURE 3 (a) Heatmap and (b) the gene expression levels of differentially expressed ATG genes between the LGG samples from TCGA database and normal samples from GTEx database. ATG, autophagy-related; GTEx, Genotype-Tissue Expression Database; LGG, lower grade glioma; TCGA, The Cancer Genome Atlas

Gene Ontology (GO) and Kyoto Encyclopedia of Genes and Genomes (KEGG) were used with the R package "ClusterProfiler" (Yu, Wang, Han, & He, 2012).

2.3 | Construction and validation of the prognostic risk score model

Univariate/multivariate Cox regression analysis was performed on DE-ATGs of the training cohort in TCGA to identify the association between the expression levels of the genes and patients' OS using the "survival" package in R (http://bioconductor.org/packages/survival/; Linden & Yarnold, 2017).

The least absolute shrinkage and selection operator (LASSO) Cox regression analysis is ideal for high-dimensional data (Tibshirani, 1997). We performed the LASSO Cox regression model to determine the optimal coefficient and to calculate the deviance likelihood. The coefficients and deviance were calculated with the "glmnet" package in R. According to each coefficient, the DE-ATGs were divided into high- and low-risk subgroups based on the median risk scores. The prognostic model for OS was calculated by multiplying the expression level of each DE-ATGs and corresponding coefficient.

To assess the efficiency of the prognostic risk score model, scatter and heat map plots have been shown as differentially significant OS. Kaplan–Meier (K-M) survival curve analysis was also

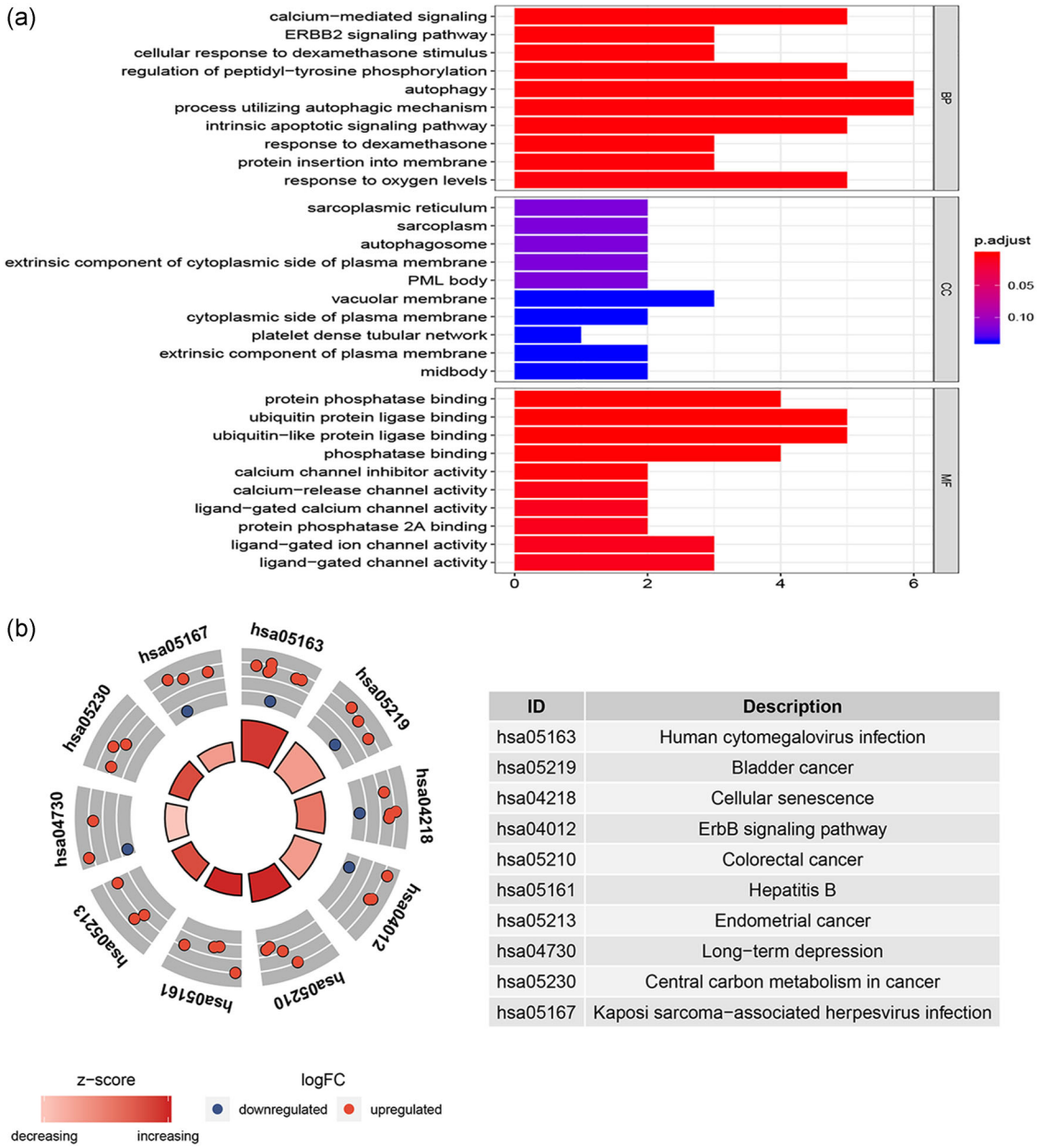

ID	Description
hsa05163	Human cytomegalovirus infection
hsa05219	Bladder cancer
hsa04218	Cellular senescence
hsa04012	ErbB signaling pathway
hsa05210	Colorectal cancer
hsa05161	Hepatitis B
hsa05213	Endometrial cancer
hsa04730	Long−term depression
hsa05230	Central carbon metabolism in cancer
hsa05167	Kaposi sarcoma−associated herpesvirus infection

FIGURE 4 The top significant categories of functional enrichment analysis in the (a) GO analysis and (b) KEGG analysis. GO, Gene Otology; KEGG, Kyoto Encyclopedia of Genes and Genomes

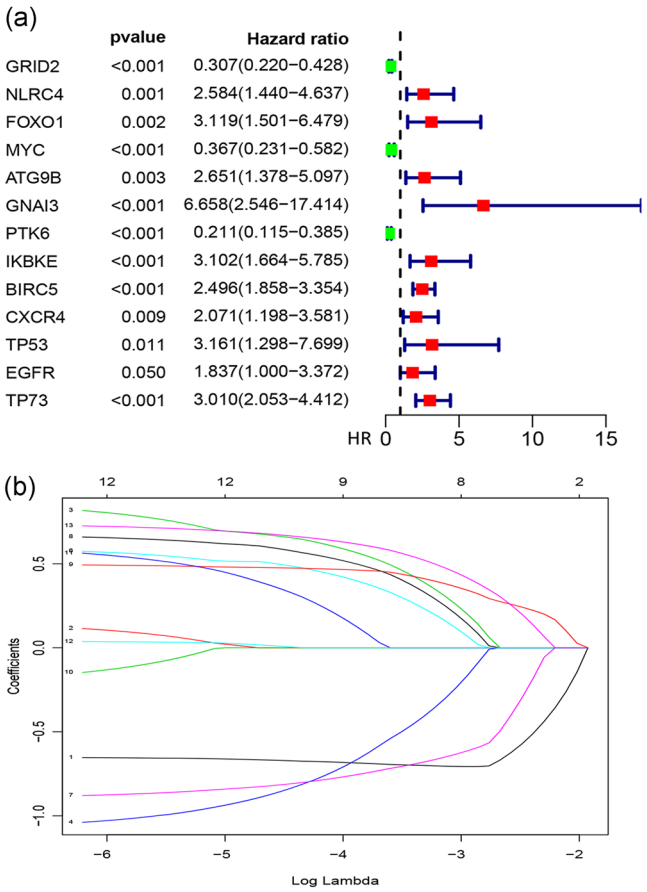

FIGURE 5 (a) The most 13 prognostic-related ATG genes. (b) Construction of prognostic signatures based on LASSO Cox analysis. ATG, autophagy-related; LASSO, least absolute shrinkage and selection operator

performed to further estimate the associations between two different subgroups and OS. Time-dependent receiver operating characteristic (ROC) curves with censored data, "timeROC" package in R (Blanche, Dartigues, & Jacqmin-Gadda, 2013), was used to generate the area under the ROC curve (AUC). The performance of the DE-ATGs-based prognostic model was validated by the CGGA validation sets 1 and 2 in similar ways.

The evaluation of autophagy signature as an independent parameter was conducted by integrating the following clinical parameters into the univariate and multivariable Cox regression analysis: age, gender, grade, IDH-mutated, O[6]-methylguanine-DNA methyltransferase-promoter-methylated, 1p19q-codeletion, and risk score.

2.4 | Construction and validation of the nomogram

All the independent prognostic factors were identified by univariate and multivariate Cox regression analysis to construct a prognostic nomogram to assess the OS probability at 1, 3, and 5 years for patients with LGG by the "rms" package in R (https://cran.r-project.org/web/packages/rms/; Qian et al., 2018).

2.5 | Gene set enrichment analysis

Gene set enrichment analysis (GSEA; http://software.broadinstitute.org/gsea/index.jsp) was performed to identify significantly enriched groups of all ATG genes, corresponding pathway, and oncogenic mechanisms (Subramanian et al., 2005). Nominal $p < .001$, FDR $q < 0.013$, and the absolute value of normal enrichment score > 1.99 of the enrichment gene sets were screened as representative.

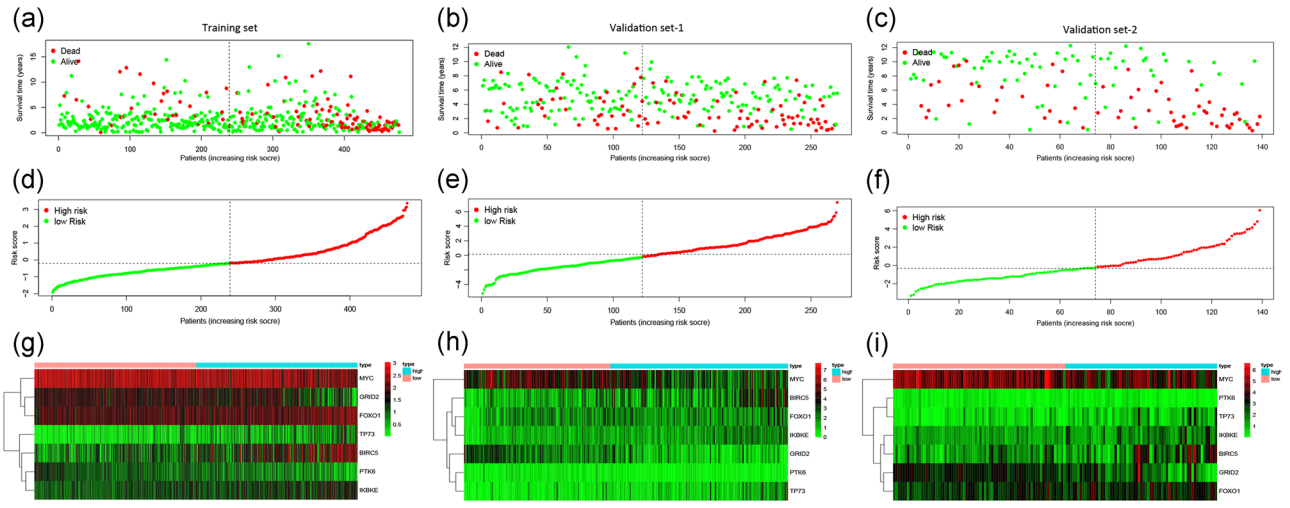

FIGURE 6 (a–c) The upper part of each dot indicates the distribution of patients' survival times and survival status. (d–f) The middle part represents the risk score curve. Color transition from green to red indicates the increasing risk score of corresponding expression level of ATG genes from low to high. (g–i) The bottom part of heat map shows the ATG signatures of every patient with LGG. ATG, autophagy-related; LGG, lower grade glioma

3 | RESULTS

3.1 | Information access and analysis flowchart

We obtained 214 ATG genes of patients with LGG from HADb (Table S1). Patients with nonapplicable clinical parameters were excluded. A total of 21 significant DE-ATGs between the LGG samples from the TCGA database ($n = 529$) and normal samples from the GTEx database ($n = 207$) were identified (Figures 2 and 3 and Table S2).

3.2 | Functional enrichment analysis

In the GO analysis, a total of 994 categories were detected. The DE-ATGs sets were enriched into biological process, cellular components, and molecular function classes, such as calcium-mediated signaling and protein phosphatase binding pathway (Figure 4a). In the KEGG analysis, a total of 46 KEGG pathways were also detected such as human cytomegalovirus infection (hsa05163), cellular senescence (hsa04218), and ErbB signaling pathway (hsa0012; Figure 4b).

3.3 | Construction and evaluation of the prognostic-related ATG-based risk score model

The most 13 ATG genes significantly correlated with prognostic-related were identified on the 21 candidate genes in the training set ($p < .05$; Figure 5a). By using LASSO Cox analysis and multivariate Cox regression analysis, a prognostic model based on seven genes was developed (Figure 5b), which was considered to be an ideal predictor with the following formula: risk score = expression level of GRID2*(−0.689) + expression level of FOXO1*(0.925) + expression level of MYC*(−0.83) + expression level of PTK6*(−0.932) + expression level of IKBKE*(−0.82) + expression level of BIRC5*(−0.626) + expression level of TP73*(−0.758) (Table S3).

Subsequently, we calculated the prognostic risk scores for all patients with LGG in the training set and the two independent validation sets. Based on the median risk score, the patients were divided into high- and low-risk subgroups, which were associated with distinct OS (Figure 6). The K-M survival curve and AUC analysis validated the performance of the prognostic model with well-performing in prognosis prediction (Figure 7).

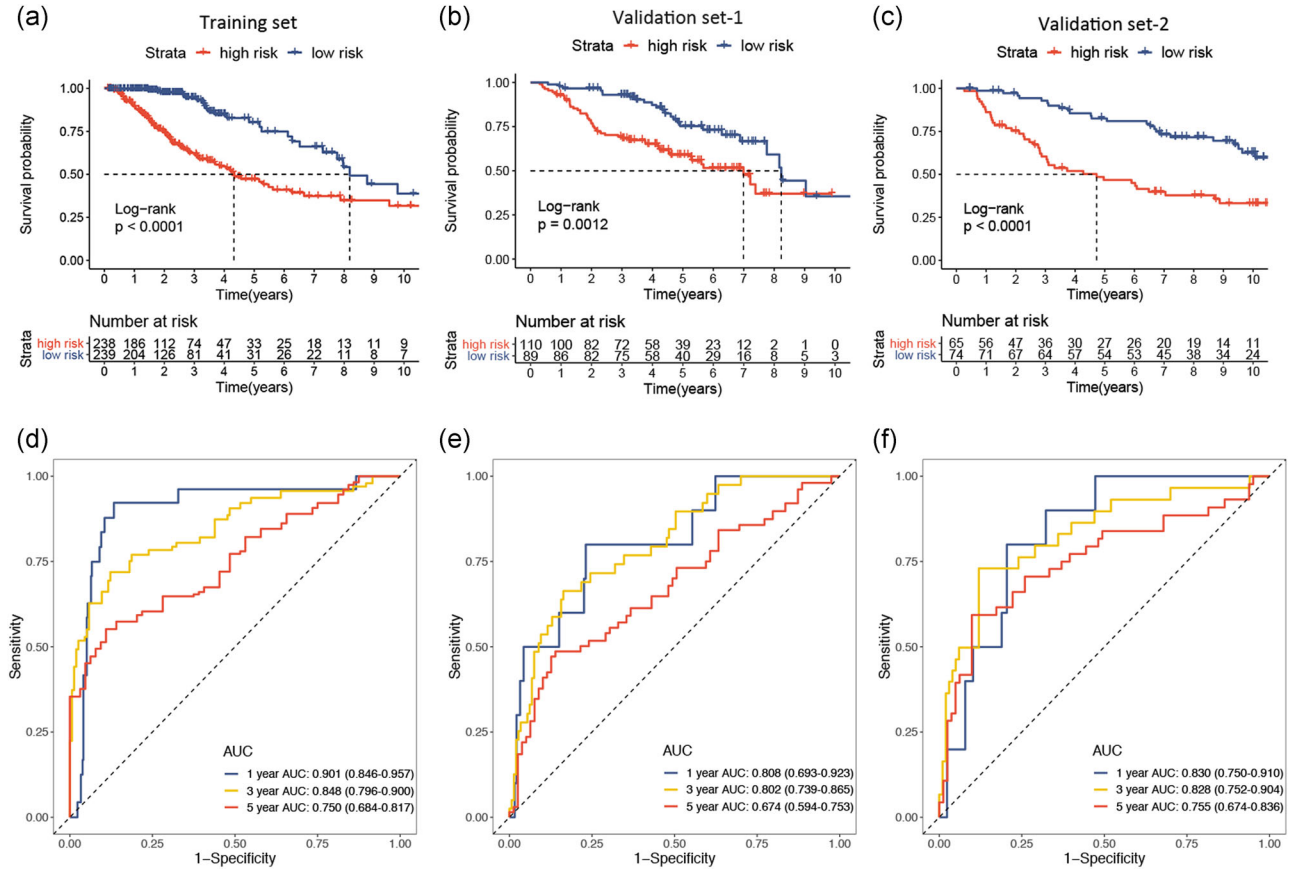

FIGURE 7 (a–c) Kaplan–Meier curves of prognostic models for high- and low-risk subgroups of patients with LGG. (d–f) Area under the ROC curves of prognostic prediction models for LGG within 1, 3, and 5 years. AUC, area under the ROC curve; LGG, lower grade glioma; ROC, receiver-operator characteristic curve

3.4 | Identification of the autophagy signature as an independent prognostic factor

The clinicopathological parameters of patients with LGG in the training set and two validation sets are shown in Table 1. Following the multivariate Cox regression and AUC analysis, the prognostic model remained a moderate and independent prognostic indicator (training set: $p = 4.09E{-}05$, AUC = 0.901; validation set-1: $p = .00069$, AUC = 0.808; validation set-2: $p = .0376$, AUC = 0.830; Table 2 and Figure 8).

3.5 | Construction and evaluation of the nomogram

A prognostic nomogram was constructed to predict the OS probability at 1, 3, and 5 years based on the training set of patients with LGG (Figure 9a). The four significantly independent parameters including age, grade, 1p19q-status, and autophagy signature were recruited in this prognostic model. The calibration plots displayed excellent predict efficiency between probability and actual OS in training set and two validation sets (Figure 9b–j).

TABLE 1 Clinicopathologic parameters of patients with LGG in the TCGA training set and CGGA validation sets

Variables (n)	Training set (*n* = 477)	Validation set-1 (*n* = 199)	Validation set-2 (*n* = 139)
Age, years			
<50	324	169	111
>50+	153	30	28
Gender			
Female	217	84	52
Male	260	115	87
Grade (WHO)			
II	230	99	92
III	247	100	47
IDH-mutated			
Yes	392	148	103
No	85	51	36
MGMT-promoter-methylated			
Yes	394	N/A	N/A
No	83	N/A	N/A
1p19q-codeletion			
Yes	157	62	52
No	320	137	87

Abbreviations: CGGA, Chinese Glioma Genome Atlas; IDH, isocitrate dehydrogenase; LGG, lower grade glioma; MGMT, O[6]-methylguanine-DNA methyltransferase; N/A, not available; TCGA, The Cancer Genome Atlas; WHO, World Health Organization.

3.6 | Gene set enrichment analysis

GSEA analyses reveal that a total of 139 underlying biological processes, especially in the group of high-risk score, including cell cycle, oocyte meiosis, pyrimidine metabolism, and focal adhesion pathway (Table S4 and Figure 10).

4 | DISCUSSION

LGGs are a type of primary neuroepithelial tumor in the cerebrum. Patients with LGG have a wide range of prognosis from 2 to 10 years based on the molecular features of the tumor and the location within the brain (Buckner et al., 2017). For an LGG, removal of the tumor accompanying with chemoradiotherapy generally allows functional survival for several years (Buckner et al., 2016). Increasing evidence shows that the classification of primary LGG depends molecular diagnosis rather than tumor grade (Baumert et al., 2016; Cancer Genome Atlas Research et al., 2015; Eckel-Passow et al., 2015; Reuss et al., 2015). These new notions should be considered in the overall management of the treatment of patient with LGG. In this study, we focused on comprehensive classification of LGG in adults on the basis of clinical parameters and molecular characteristics composed of WHO Grades II and III gliomas, including the histological types of astrocytoma, oligoastrocytoma, and oligodendroglioma, to predict OS.

Recent developments in high-throughput whole genome-sequencing technologies have promoted the identification of novel autophagy signatures that allow for further exploration of the molecular pathogenesis of LGG. Several studies have identified prognostic signatures by combining multiple genes for glioma. For example, Liu et al. (2019) identified five novel prognostic pseudogenes capable of predicting patients with LGG survival based on a risk score model. C. Zhang et al. (2019) established a four-gene signature based on the chr1p/19q codeletion in patients with LGG. Zeng et al. (2018) developed a three-gene prognostic signature by an integrated analysis of genome-wide methylation and gene expression data. Xiao et al. (2020) also reported a three-gene model of predicting short- and long-term survival of patients with LGG. Although these signatures have the potential to predict LGG patients' survival, the sample sizes of some studies were not enough and it is insufficient to prove the signatures stability for limit samples and validity. In this study, we integrated the ATG genes and clinical information of patients with LGG to identify prognosis-related autophagy signatures and construct prognostic model that could stratify patients with LGG into subgroups with distinct OS for uncovering potential molecular biomarkers. The prognostic model based on these signatures had satisfactory performance in prognostic prediction under two other validation sets. A nomogram composed of clinical parameters and risk score also performs well in prediction of OS probability. Our model was validated and possessed a stable predictive efficacy in two validation sets. Moreover, comparing with

TABLE 2 Cox regression analysis of clinical characteristics and autophagy signature of patients with LGG in the TCGA training set and two CGGA validation sets

	Training set in TCGA (*n* = 477)				Validation set-1 in CGGA (*n* = 199)				Validation set-2 in CGGA (*n* = 139)			
	Univariate		Multivariate		Univariate		Multivariate		Univariate		Multivariate	
Characteristics	HR (95% CI)	*p*	HR (95% CI)	*p*	HR (95% CI)	*p*	HR (95% CI)	*p*	HR (95% CI)	*p*	HR (95% CI)	*p*
Age, years												
<50	1.059 (1.044–1.075)	8.46E−15	1.045 (1.028–1.063)	2.42E−07	1.004 (0.982–1.026)	.73997	1.018 (0.995–1.042)	.12367	1.052 (1.025–1.080)	.00014	1.028 (1.002–1.055)	.0374
≥50												
Gender												
Female	1.044 (0.729–1.497)	.81313	1.166 (0.802–1.695)	.421641	1.480 (0.914–2.395)	.11069	2.144 (1.264–3.637)	.00468	0.666 (0.403–1.101)	.11261	0.662 (0.386–1.136)	.1341
Male												
Grade												
I	3.317 (2.230–4.934)	3.24E−09	1.737 (1.126–2.680)	.012545	3.180 (1.876–5.393)	1.75E−05	3.113 (1.784–5.432)	.00006	3.477 (2.091–5.780)	1.56E−06	2.620 (1.377–4.987)	.0033
II												
IDH-mutated												
Yes	0.148 (0.102–0.216)	2.40E−23	0.668 (0.333–1.337)	.254055	0.327 (0.200–0.533)	7.44E−06	0.533 (0.278–1.023)	.05870				
No									0.305 (0.180–0.515)	8.85E−06	1.453 (0.681–3.099)	.3338
MGMT-promoter-methylated												
Yes	0.377 (0.257–0.554)	7.06E−07	1.045 (0.626–1.745)	.865637	N/A	N/A	N/A	N/A	N/A	N/A	N/A	N/A
No												
1p19q-codeletion												
Yes	0.373 (0.230–0.602)	5.61E−05	0.478 (0.279–0.821)	.007444	0.190 (0.091–0.396)	9.64E−06	0.272 (0.125–0.589)	.00096	0.155 (0.076–0.316)	3.11E−07	0.206 (0.093–0.457)	.0001
No												
Risk score												
High	2.738 (2.292–3.271)	1.15E−28	1.714 (1.325–2.217)	4.09E−05	1.424 (1.269–1.598)	1.84E−09	1.287 (1.113–1.489)	.00069	1.404 (1.235–1.596)	2.16E−07	1.225 (1.012–1.484)	.0376
Low												

Abbreviations: CGGA, Chinese Glioma Genome Atlas; CI, confidence interval; HR, hazard ratio; IDH, isocitrate dehydrogenase; LGG, lower grade glioma; MGMT, O[6]-methylguanine-DNA methyltransferase; N/A, not available; TCGA, The Cancer Genome Atlas.

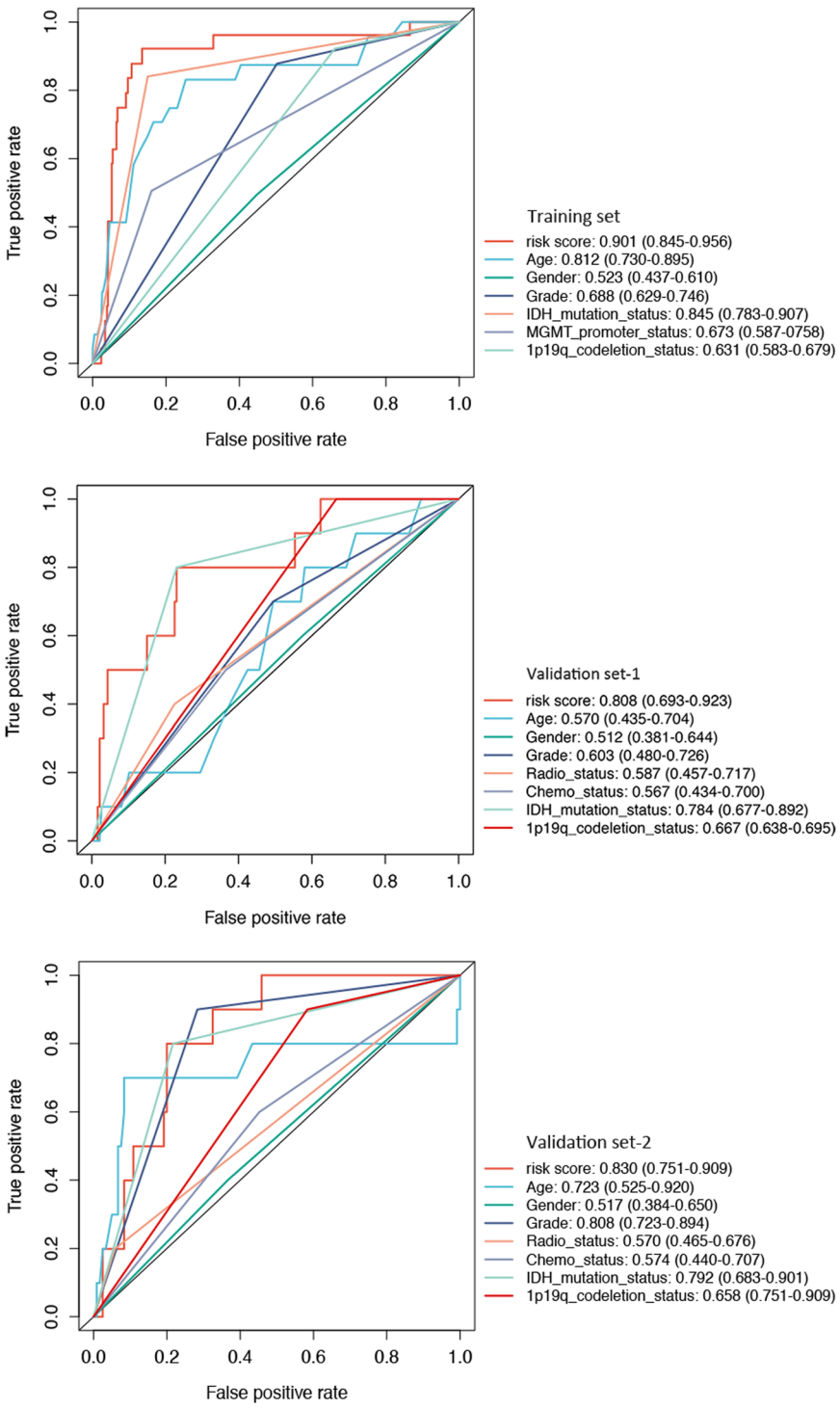

FIGURE 8 Area under the ROC curves of risk scores and clinicopathologic parameters for patients with LGG in training set and two validation sets. LGG, lower grade glioma; ROC, receiver-operator characteristic curve

other corresponding studies, our model showed satisfactory performance in predicting the 1-, 3-, and 5-year survival of patients with LGG through time-dependent ROC curve analysis. Therefore, we established a promising prognostic model to assist individualized survival prediction of patients with LGG.

ATG pathway selectively targets intracellular microbes, dysfunctional organelles, and pathogenic proteins (Levine & Kroemer, 2019). This process is conserved in all eukaryotic organisms. It is essential for cellular homeostasis, stress proteins, and organismal adaptation to environmental stress (Mizushima & Komatsu, 2011). To date, 16 "core" ATG genes have been identified, which are commonly used by both nonselective and selective macroautophagy, and the others are exclusive to the selective autophagy of various organelles, including mitochondria, endoplasmic reticulum (ER), lipid droplets, peroxisomes, ribosomes, and the nucleus (Nakatogawa, Suzuki, Kamada, & Ohsumi, 2009; Parzych, Ariosa, Mari, & Klionsky, 2018).

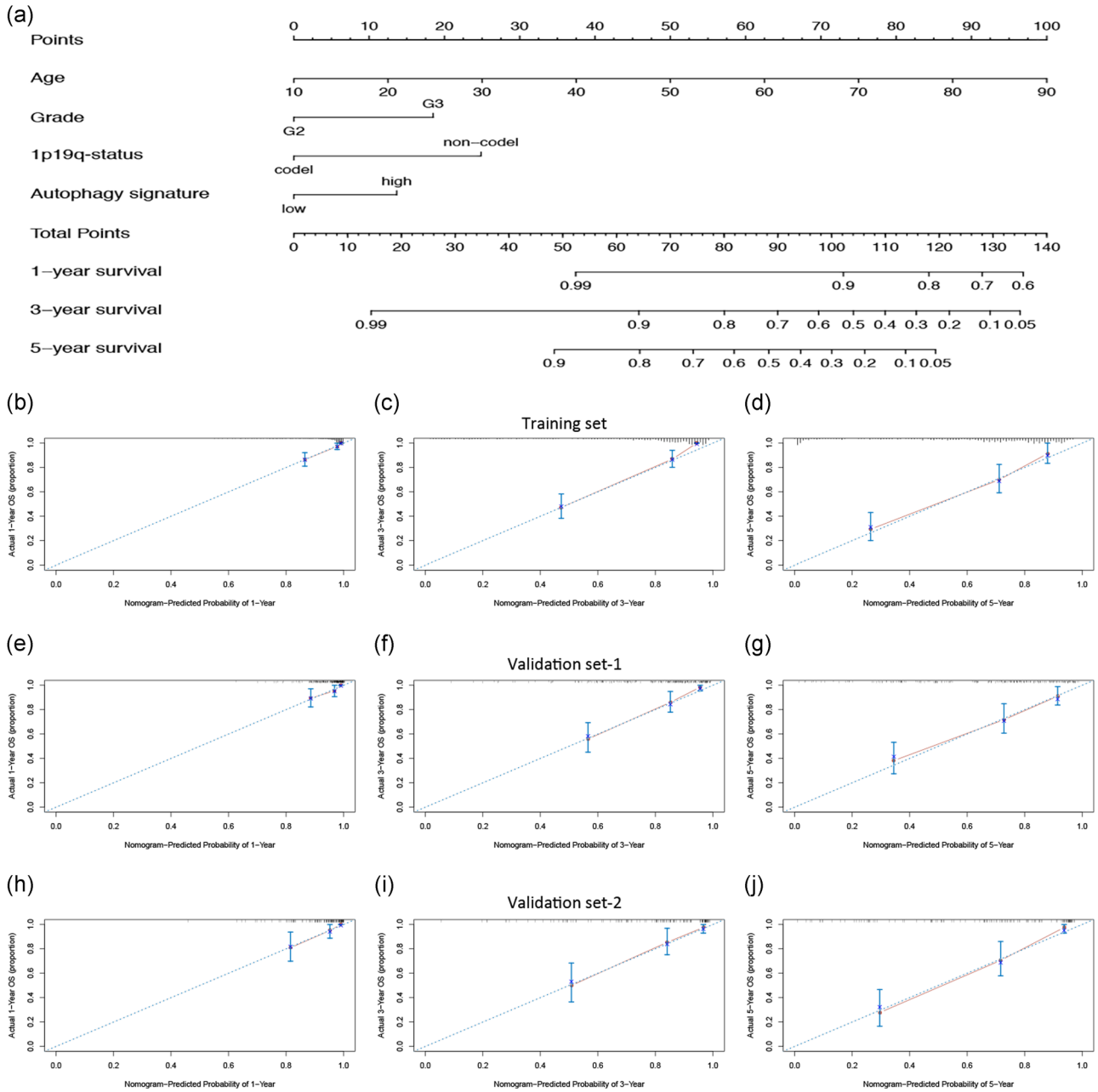

FIGURE 9 (a) A prognostic nomogram was constructed to predict the OS probability based on the training set of patients with LGG. (b–j) The calibration plots validated excellent predict efficiency. LGG, lower grade glioma; OS, overall survival

The numerous links between mutations in selective autophagy genes and human diseases emphasize the physiological importance of selective autophagy. The role of autophagy in promoting genomic stability is consistent with its role in tumor suppression. Autophagy acts to dampen protumorigenic inflammation and to enhance adaptive immunity in myeloid cells by enhancing antitumor cytotoxic T lymphocyte responses and contributing to the antitumor efficacy of radiochemical therapy (Drake, Springer, Poole, Kim, & Macleod, 2017; Galluzzi, Buque, Kepp, Zitvogel, & Kroemer, 2017; Wu et al., 2017; Yan et al., 2016; Z. Zhang et al., 2019). Wu et al. (2017) reported that the role of autophagy in the antiangiogenic therapy could improve the susceptibility of bevacizumab. In addition, there has been some hypotheses that autophagy inhibitors could enhance the benefits of TMZ chemosensitivity in the treatment of aggressive gliomas (Yan et al., 2016). In parallel with the antitumor efficacy, numerous studies have demonstrated protumorigenic roles of autophagy, primarily in cancers driven by KRAS that require high cellular metabolic activity to sustain survival (Kimmelman & White, 2017), and ATG genes lead to maintain tumor cellular energy production (Razaghi, Heimann, Schaeffer, & Gibson, 2018). Therefore, autophagy plays an important role in cancer, both in protecting against cancer as well as potentially contributing to the growth of

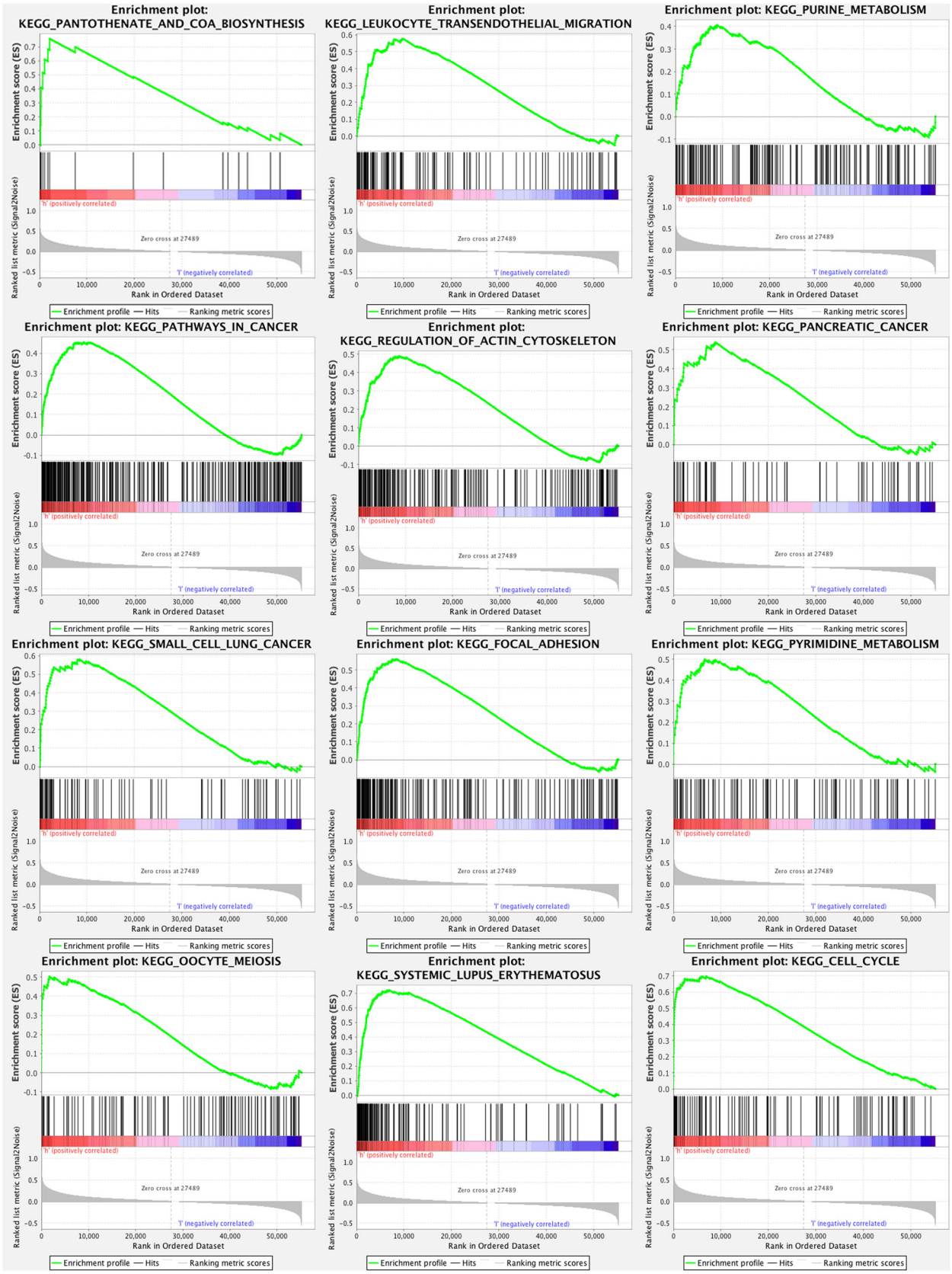

FIGURE 10 GSEA analyses reveal underlying biological processes on ATG genes. ATG, autophagy-related; GSEA, gene set enrichment analysis

cancer. Further progress in our understanding of autophagy biology would clarify the roles of the process in the growth of cancer relating to the pathophysiological effects at the cellular and tissue level.

Here, we systematically identified seven prognosis-related ATG genes including GRID2, FOXO1, MYC, TP73, IKBKE, PTK6, and BIRC5. It is potential to be a novel therapeutic targets and prognostic predictors in LGG. The protein encoded by *GRID2* gene is a member of the family of ionotropic glutamate receptors that act as an excitatory neurotransmitter in the central nervous system. Previous study reported that biallelic deletions of *GRID2* lead to a syndrome of cerebellar ataxia and tonic upgaze in humans, which indicate an evolutionarily unique role for *GRID2* in the human cerebellum (Hills et al., 2013). The *FoxO1* gene belongs to the forkhead family of transcription factors that are characterized by a distinct forkhead domain. It has been reported that silencing of *Akt1* by decreasing phosphorylated *Foxo1* and inducing the expression of *Foxo1* inhibited the growth and invasion of glioma cells (Que et al., 2015). Overexpression of *FoxO1* was able to enhance the etoposide-induced apoptosis pathway in glioma (Ni et al., 2019). In addition, the features of activated in *mTORC2* signaling, *c-Myc* levels, and acetylated *FoxO1* are highly intercorrelated in clinical glioma samples and with shorter survival of patients with GBM (Masui et al., 2013). MYC is a family of regulator genes and proto-oncogenes that code for transcription factors, which is viewed as a promising target for anticancer drugs. However, due to several undruggable features, any anticancer drugs for *Myc* will require acting on the messenger RNA rather than the protein itself. As a prognostic biomarker, the long noncoding RNA *TP73-AS1* with high expression in glioma cells and promoting temozolomide (TMZ) resistance in glioblastoma cancer stem cells with poor prognosis have been reported (Mazor et al., 2019). Due to *IKBKE* overexpressing in human gliomas, the downregulation of *IKBKE* inhibits the proliferative and invasive abilities of glioma cells (Tian et al., 2015). Similarly, regulating IKBKE/nuclear factor-κB signaling axis by inhibiting *PLK4* increases TMZ sensitivity and suppresses glioma proliferation via therapeutic targeting (Z. Zhang et al., 2019). The above-mentioned studies are consistent with our results. The role of *Ptk6* and *BIRC5* in neurologic tumors are still unclear and need further research for novel therapeutic target.

Nomograms have been widely used in clinical study since they provide an intuitive visual presentation (Harrell, Lee, & Mark, 1996). A nomogram, in this study, with the age, grade, 1p19q-status, and autophagy signature was constructed to perform individualized survival prediction more precisely. The calibration plots based on the training and validation sets exhibited excellent consistency between the actual survival (CGGA) and the predicted survival (TCGA).

Limitations inevitably impact on our study. There were a limited number of patients with LGG with intact clinical information recruited in our analysis. More datasets of whole genome sequencing in glioma disease are needed to validate prognostic model and potential biomarkers. Further experiments on the functions and mechanisms are needed to validate the efficiency of these autophagy signatures in LGG progression.

Finally, we identified the prognostic model and nomogram, based on seven favorable autophagy signatures, performed well in prediction of OS probability for patients with LGG. According to our study, several potential biomarkers could be elucidated from further validations. It may also be beneficial to promote prognosis prediction and therapeutic target.

5 | CONCLUSIONS

In summary, the current study established a prognostic model based on seven survival-associated ATG genes and a promising prognostic nomogram based on autophagy signature and clinical characteristics, which is valuable for clinical glioma management. The further identification of promising biomarker will facilitate the ongoing effort on exploration of autophagy mechanisms and therapeutic target in LGG patients.

ACKNOWLEDGMENTS

The authors would like to thank The Cancer Genome Atlas and Chinese Glioma Genome Atlas databases for the availability of the data.

CONFLICT OF INTERESTS

The authors declare that there are no conflict of interests.

AUTHOR CONTRIBUTIONS

C. W. and H. H. contributed to conceptualization and methodology. C. W., J. Q., and Y. L. contributed to software, validation, and data curation. Original draft preparation was done by J. Q. and C. W. J. Q. and S. C. reviewed and edited the manuscript. Supervision was dine by Y. C. and L. H. L. H. did the project administration. All authors approved the final manuscript.

DATA AVAILABILITY STATEMENT

The data of lower grade glioma in this study were downloaded from The Cancer Genome Atlas and the Chinese Glioma Genome Atlas. The data of the normal brain tissues were downloaded from Genotype-Tissue Expression Database. All autophagy-related genes were obtained in Human Autophagy Database.

ORCID

Lijun Hou http://orcid.org/0000-0002-1803-3201

REFERENCES

Bauchet, L., & Ostrom, Q. T. (2019). Epidemiology and molecular epidemiology. *Neurosurgery Clinics of North America*, *30*(1), 1–16. https://doi.org/10.1016/j.nec.2018.08.010

Baumert, B. G., Hegi, M. E., van den Bent, M. J., von Deimling, A., Gorlia, T., Hoang-Xuan, K., … Stupp, R. (2016). Temozolomide chemotherapy versus radiotherapy in high-risk low-grade glioma (EORTC 22033-26033): A randomised, open-label, phase 3 intergroup study. *The Lancet Oncology*, *17*(11), 1521–1532. https://doi.org/10.1016/S1470-2045(16)30313-8

Benjamini, Y., & Hochberg, Y. (1995). Controlling the false discovery rate: A practical and powerful approach to multiple testing. *Journal of the Royal Statistical Society: Series B (Methodological)*, *57*(1), 289–300. https://doi.org/10.1111/j.2517-6161.1995.tb02031.x

van den Bent, M. J. (2010). Interobserver variation of the histopathological diagnosis in clinical trials on glioma: A clinician's perspective. *Acta Neuropathologica*, *120*(3), 297–304. https://doi.org/10.1007/s00401-010-0725-7

Blanche, P., Dartigues, J. F., & Jacqmin-Gadda, H. (2013). Estimating and comparing time-dependent areas under receiver operating characteristic curves for censored event times with competing risks. *Statistics in Medicine*, *32*(30), 5381–5397. https://doi.org/10.1002/sim.5958

Bready, D., & Placantonakis, D. G. (2019). Molecular pathogenesis of low-grade glioma. *Neurosurgery Clinics of North America*, *30*(1), 17–25. https://doi.org/10.1016/j.nec.2018.08.011

Buckner, J. C., Giannini, C., Eckel-Passow, J., Lachance, D., Parney, I., Laack, N., & Jenkins, R. (2017). Management of diffuse low-grade gliomas in adults—Use of molecular diagnostics. *Nature Reviews Neurology*, *13*(6), 340–351. https://doi.org/10.1038/nrneurol.2017.54

Buckner, J. C., Shaw, E. G., Pugh, S. L., Chakravarti, A., Gilbert, M. R., Barger, G. R., … Curran, W. J., Jr. (2016). Radiation plus procarbazine, CCNU, and vincristine in low-grade glioma. *New England Journal of Medicine*, *374*(14), 1344–1355. https://doi.org/10.1056/NEJMoa1500925

Cancer Genome Atlas Research Network (2015). Comprehensive, integrative genomic analysis of diffuse lower-grade gliomas. *New England Journal of Medicine*, *372*(26), 2481–2498. https://doi.org/10.1056/NEJMoa1402121

Drake, L. E., Springer, M. Z., Poole, L. P., Kim, C. J., & Macleod, K. F. (2017). Expanding perspectives on the significance of mitophagy in cancer. *Seminars in Cancer Biology*, *47*, 110–124. https://doi.org/10.1016/j.semcancer.2017.04.008

Eckel-Passow, J. E., Lachance, D. H., Molinaro, A. M., Walsh, K. M., Decker, P. A., Sicotte, H., … Jenkins, R. B. (2015). Glioma Groups Based on 1p/19q, IDH, and TERT Promoter Mutations in Tumors. *New England Journal of Medicine*, *372*(26), 2499–2508. https://doi.org/10.1056/NEJMoa1407279

Furnari, F. B., Fenton, T., Bachoo, R. M., Mukasa, A., Stommel, J. M., Stegh, A., … Cavenee, W. K. (2007). Malignant astrocytic glioma: Genetics, biology, and paths to treatment. *Genes and Development*, *21*(21), 2683–2710. https://doi.org/10.1101/gad.1596707

Galluzzi, L., Buque, A., Kepp, O., Zitvogel, L., & Kroemer, G. (2017). Immunogenic cell death in cancer and infectious disease. *Nature Reviews Immunology*, *17*(2), 97–111. https://doi.org/10.1038/nri.2016.107

Harrell, F. E., Jr., Lee, K. L., & Mark, D. B. (1996). Multivariable prognostic models: Issues in developing models, evaluating assumptions and adequacy, and measuring and reducing errors. *Statistics in Medicine*, *15*(4), 361–387. https://doi.org/10.1002/(SICI)1097-0258(19960229)15:4<361::AID-SIM168>3.0.CO;2-4

Hills, L. B., Masri, A., Konno, K., Kakegawa, W., Lam, A. T., Lim-Melia, E., … Mochida, G. H. (2013). Deletions in GRID2 lead to a recessive syndrome of cerebellar ataxia and tonic upgaze in humans. *Neurology*, *81*(16), 1378–1386. https://doi.org/10.1212/WNL.0b013e3182a841a3

Kimmelman, A. C., & White, E. (2017). Autophagy and tumor metabolism. *Cell Metabolism*, *25*(5), 1037–1043. https://doi.org/10.1016/j.cmet.2017.04.004

Levine, B., & Kroemer, G. (2019). Biological functions of autophagy genes: A disease perspective. *Cell*, *176*(1-2), 11–42. https://doi.org/10.1016/j.cell.2018.09.048

Linden, A., & Yarnold, P. R. (2017). Modeling time-to-event (survival) data using classification tree analysis. *Journal of Evaluation in Clinical Practice*, *23*(6), 1299–1308. https://doi.org/10.1111/jep.12779

Liu, B., Liu, J., Liu, K., Huang, H., Li, Y., Hu, X., … Cheng, Q. (2019). A prognostic signature of five pseudogenes for predicting lower-grade gliomas. *Biomedicine & Pharmacotherapy*, *117*, 109116. https://doi.org/10.1016/j.biopha.2019.109116

Masui, K., Tanaka, K., Akhavan, D., Babic, I., Gini, B., Matsutani, T., … Mischel, P. S. (2013). mTOR complex 2 controls glycolytic metabolism in glioblastoma through FoxO acetylation and upregulation of c-Myc. *Cell Metabolism*, *18*(5), 726–739. https://doi.org/10.1016/j.cmet.2013.09.013

Mazor, G., Levin, L., Picard, D., Ahmadov, U., Caren, H., Borkhardt, A., … Rotblat, B. (2019). The lncRNA TP73-AS1 is linked to aggressiveness in glioblastoma and promotes temozolomide resistance in glioblastoma cancer stem cells. *Cell Death & Disease*, *10*(3), 246. https://doi.org/10.1038/s41419-019-1477-5

Mizushima, N. (2018). A brief history of autophagy from cell biology to physiology and disease. *Nature Cell Biology*, *20*(5), 521–527. https://doi.org/10.1038/s41556-018-0092-5

Mizushima, N., & Komatsu, M. (2011). Autophagy: Renovation of cells and tissues. *Cell*, *147*(4), 728–741. https://doi.org/10.1016/j.cell.2011.10.026

Moussay, E., Kaoma, T., Baginska, J., Muller, A., Van Moer, K., Nicot, N., … Janji, B. (2011). The acquisition of resistance to TNFalpha in breast cancer cells is associated with constitutive activation of autophagy as revealed by a transcriptome analysis using a custom microarray. *Autophagy*, *7*(7), 760–770. https://doi.org/10.4161/auto.7.7.15454

Nakatogawa, H., Suzuki, K., Kamada, Y., & Ohsumi, Y. (2009). Dynamics and diversity in autophagy mechanisms: Lessons from yeast. *Nature Reviews Molecular Cell Biology*, *10*(7), 458–467. https://doi.org/10.1038/nrm2708

Ni, W., Luo, L., Zuo, P., Li, R., Xu, X., Wen, F., & Hu, D. (2019). miR-374a inhibitor enhances etoposide-induced cytotoxicity against glioma cells through upregulation of FOXO1. *Oncology Research*, *27*(6), 703–712. https://doi.org/10.3727/096504018X15426775024905

Parzych, K. R., Ariosa, A., Mari, M., & Klionsky, D. J. (2018). A newly characterized vacuolar serine carboxypeptidase, Atg42/Ybr139w, is required for normal vacuole function and the terminal steps of autophagy in the yeast *Saccharomyces cerevisiae*. *Molecular Biology of the Cell*, *29*(9), 1089–1099. https://doi.org/10.1091/mbc.E17-08-0516

Petalidis, L. P., Oulas, A., Backlund, M., Wayland, M. T., Liu, L., Plant, K., … Collins, V. P. (2008). Improved grading and survival prediction of human astrocytic brain tumors by artificial neural network analysis of gene expression microarray data. *Molecular Cancer Therapeutics*, *7*(5), 1013–1024. https://doi.org/10.1158/1535-7163.MCT-07-0177

Qian, Z., Li, Y., Fan, X., Zhang, C., Wang, Y., Jiang, T., & Liu, X. (2018). Prognostic value of a microRNA signature as a novel biomarker in patients with lower-grade gliomas. *Journal of Neuro-Oncology*, *137*(1), 127–137. https://doi.org/10.1007/s11060-017-2704-5

Que, T., Song, Y., Liu, Z., Zheng, S., Long, H., Li, Z., … Qi, S. (2015). Decreased miRNA-637 is an unfavorable prognosis marker and promotes glioma cell growth, migration and invasion via direct targeting Akt1. *Oncogene*, *34*(38), 4952–4963. https://doi.org/10.1038/onc.2014.419

Rao, S. A., Santosh, V., & Somasundaram, K. (2010). Genome-wide expression profiling identifies deregulated miRNAs in malignant astrocytoma. *Modern Pathology*, *23*(10), 1404–1417. https://doi.org/10.1038/modpathol.2010.135

Razaghi, A., Heimann, K., Schaeffer, P. M., & Gibson, S. B. (2018). Negative regulators of cell death pathways in cancer: Perspective on biomarkers and targeted therapies. *Apoptosis*, *23*(2), 93–112. https://doi.org/10.1007/s10495-018-1440-4

Reuss, D. E., Kratz, A., Sahm, F., Capper, D., Schrimpf, D., Koelsche, C., … von Deimling, A. (2015). Adult IDH wild type astrocytomas biologically and clinically resolve into other tumor entities. *Acta Neuropathologica*, *130*(3), 407–417. https://doi.org/10.1007/s00401-015-1454-8

Subramanian, A., Tamayo, P., Mootha, V. K., Mukherjee, S., Ebert, B. L., Gillette, M. A., … Mesirov, J. P. (2005). Gene set enrichment analysis:

A knowledge-based approach for interpreting genome-wide expression profiles. *Proceedings of the National Academy of Sciences of the United States of America*, *102*(43), 15545–15550. https://doi.org/10.1073/pnas.0506580102

Tian, Y., Hao, S., Ye, M., Zhang, A., Nan, Y., Wang, G., … Zhong, Y. (2015). MicroRNAs let-7b/i suppress human glioma cell invasion and migration by targeting IKBKE directly. *Biochemical and Biophysical Research Communications*, *458*(2), 307–312. https://doi.org/10.1016/j.bbrc.2015.01.105

Tibshirani, R. (1997). The lasso method for variable selection in the Cox model. *Statistics in Medicine*, *16*(4), 385–395. https://doi.org/10.1002/(sici)1097-0258(19970228)16:4<385::aid-sim380>3.0.co;2-3

Ulasov, I., Fares, J., Timashev, P., & Lesniak, M. S. (2019). Editing cytoprotective autophagy in glioma: An unfulfilled potential for therapy. *Trends in Molecular Medicine*, *26*, 252–262. https://doi.org/10.1016/j.molmed.2019.11.001.

Wang, Z., Gao, L., Guo, X., Feng, C., Deng, K., Lian, W., & Xing, B. (2019). Identification of microRNAs associated with the aggressiveness of prolactin pituitary tumors using bioinformatic analysis. *Oncology Reports*, *42*(2), 533–548. https://doi.org/10.3892/or.2019.7173

Wu, H. B., Yang, S., Weng, H. -Y., Chen, Q., Zhao, X. L., Fu, W. J., … Bian, X. -W. (2017). Autophagy-induced KDR/VEGFR-2 activation promotes the formation of vasculogenic mimicry by glioma stem cells. *Autophagy*, *13*(9), 1528–1542. https://doi.org/10.1080/15548627.2017.1336277

Xiao, K., Liu, Q., Peng, G., Su, J., Qin, C. Y., & Wang, X. Y. (2020). Identification and validation of a three-gene signature as a candidate prognostic biomarker for lower grade glioma. *PeerJ*, *8*, e8312. https://doi.org/10.7717/peerj.8312

Yan, Y., Xu, Z., Dai, S., Qian, L., Sun, L., & Gong, Z. (2016). Targeting autophagy to sensitive glioma to temozolomide treatment. *Journal of Experimental & Clinical Cancer Research*, *35*, 23. https://doi.org/10.1186/s13046-016-0303-5

Yu, G., Wang, L. G., Han, Y., & He, Q. Y. (2012). clusterProfiler: An R package for comparing biological themes among gene clusters. *OMICS*, *16*(5), 284–287. https://doi.org/10.1089/omi.2011.0118

Zeng, W. J., Yang, Y. L., Liu, Z. Z., Wen, Z. P., Chen, Y. H., Hu, X. L., … Chen, X. P. (2018). Integrative analysis of dna methylation and gene expression identify a three-gene signature for predicting prognosis in lower-grade gliomas. *Cellular Physiology and Biochemistry*, *47*(1), 428–439. https://doi.org/10.1159/000489954

Zhang, C., Yu, R., Li, Z., Song, H., Zang, D., Deng, M., … Qu, X. (2019). Comprehensive analysis of genes based on chr1p/19q co-deletion reveals a robust 4-gene prognostic signature for lower grade glioma. *Cancer Management and Research*, *11*, 4971–4984. https://doi.org/10.2147/CMAR.S199396

Zhang, Z., Wang, Z., Huang, K., Liu, Y., Wei, C., Zhou, J., … Han, L. (2019). PLK4 is a determinant of temozolomide sensitivity through phosphorylation of IKBKE in glioblastoma. *Cancer Letters*, *443*, 91–107. https://doi.org/10.1016/j.canlet.2018.11.034

SUPPORTING INFORMATION

Additional supporting information may be found online in the Supporting Information section.

How to cite this article: Wang C, Qiu J, Chen S, et al. Prognostic model and nomogram construction based on autophagy signatures in lower grade glioma. *J Cell Physiol*. 2020;1–14. https://doi.org/10.1002/jcp.29837